

SANDIA REPORT

SAND2004-5276

Unlimited Release

Printed November, 2004

Self-Assembled Ordered Carbon-Nanotube Arrays and Membranes

M. P. Siegal, D. L. Overmyer, W. G. Yelton

Prepared by
Sandia National Laboratories
Albuquerque, New Mexico 87185 and Livermore, California 94550

Sandia is a multiprogram laboratory operated by Sandia Corporation, a Lockheed Martin Company, for the United States Department of Energy's National Nuclear Security Administration under Contract DE-AC04-94AL85000.

Approved for public release; further dissemination unlimited.



Sandia National Laboratories

Issued by Sandia National Laboratories, operated for the United States Department of Energy by Sandia Corporation.

NOTICE: This report was prepared as an account of work sponsored by an agency of the United States Government. Neither the United States Government, nor any agency thereof, nor any of their employees, nor any of their contractors, subcontractors, or their employees, make any warranty, express or implied, or assume any legal liability or responsibility for the accuracy, completeness, or usefulness of any information, apparatus, product, or process disclosed, or represent that its use would not infringe privately owned rights. Reference herein to any specific commercial product, process, or service by trade name, trademark, manufacturer, or otherwise, does not necessarily constitute or imply its endorsement, recommendation, or favoring by the United States Government, any agency thereof, or any of their contractors or subcontractors. The views and opinions expressed herein do not necessarily state or reflect those of the United States Government, any agency thereof, or any of their contractors.

Printed in the United States of America. This report has been reproduced directly from the best available copy.

Available to DOE and DOE contractors from
U.S. Department of Energy
Office of Scientific and Technical Information
P.O. Box 62
Oak Ridge, TN 37831

Telephone: (865)576-8401
Facsimile: (865)576-5728
E-Mail: reports@adonis.osti.gov
Online ordering: <http://www.osti.gov/bridge>

Available to the public from
U.S. Department of Commerce
National Technical Information Service
5285 Port Royal Rd
Springfield, VA 22161

Telephone: (800)553-6847
Facsimile: (703)605-6900
E-Mail: orders@ntis.fedworld.gov
Online order: <http://www.ntis.gov/help/ordermethods.asp?loc=7-4-0#online>



Self-Assembled Ordered Carbon-Nanotube Arrays and Membranes

M. P. Siegal and D. L. Overmyer
Advanced Materials Sciences Department

W. G. Yelton
Photonic Microsystems Technologies Department

Sandia National Laboratories
P.O. Box 5800
Albuquerque, NM 87185-1421

ABSTRACT

Imagine free-standing flexible membranes with highly-aligned arrays of carbon nanotubes (CNTs) running through their thickness. Perhaps with both ends of the CNTs open for highly-controlled nanofiltration? Or CNTs at heights uniformly above a polymer membrane for a flexible array of nanoelectrodes or field-emitters? How about CNT films with incredible amounts of accessible surface area for analyte adsorption? These self-assembled crystalline nanotubes consist of multiple layers of graphene sheets rolled into concentric cylinders. Tube diameters (3-300 nm), inner-bore diameters (2-15 nm), and lengths (nanometers – microns) are controlled to tailor physical, mechanical, and chemical properties. We proposed to explore growth and characterize nanotube arrays to help determine their exciting functionality for Sandia applications. Thermal chemical vapor deposition growth in a furnace nucleates from a metal catalyst. Ordered arrays grow using templates from self-assembled hexagonal arrays of nanopores in anodized-aluminum oxide. Polymeric-binders can mechanically hold the CNTs in place for polishing, lift-off, and membrane formation.

The stiffness, electrical and thermal conductivities of CNTs make them ideally suited for a wide-variety of possible applications. Large-area, highly-accessible gas-adsorbing carbon surfaces, superb cold-cathode field-emission, and unique nanoscale geometries can lead to advanced microsensors using analyte adsorption, arrays of functionalized nanoelectrodes for enhanced electrochemical detection of biological/explosive compounds, or mass-ionizers for gas-phase detection. Materials studies involving membrane formation may lead to exciting breakthroughs in nanofiltration/nanochromatography for the separation of chemical and biological agents. With controlled nanofilter sizes, ultrafiltration will be viable to separate and preconcentrate viruses and many strains of bacteria for “down-stream” analysis.

Acknowledgements

The authors thank D. R. Tallant for Raman analysis, F. H. Kaatz for help setting up the nanotube CVD growth apparatus, P. P. Provencio for performing some TEM analysis, and A. Rowen for assist with Al film anodization for template formation. Supported by Laboratory Directed Research and Development, Sandia is a multiprogram laboratory operated by Sandia Corporation, a Lockheed Martin Company, or the United States Department of Energy's National Nuclear Security Administration under contract DE-AC04-94AL85000.

Table of Contents

Abstract	iii
Acknowledgements	iv
I. Introduction	1
II. Controlling CNT Diameters	3
III. Controlling the Site Density of Multiwall CNTs	9
IV. AAO Template Formation	15
V. Summary	17
VI. Publications, Presentations and Patent Disclosures	18
Distribution List	19

Figures

1.1 Aligned CNTs	1
1.2 CNT array	2
2.1 SEMs of CNTs grown vs. temperature	5
2.2 CNT diameters vs. growth temperature	5
2.3 RBS spectrum for CNT/Ni/W/Si(100)	6
2.4 Carbon atom areal density vs. growth temperature	7
3.1 Heat of formation of various hydrocarbon gases	10
3.2 SEMs of CNTs vs. hydrocarbon gas	10
3.3 Residual stress of W and Ni vs. sputter conditions	11
3.4 SEMs of CNTs vs. metal layer stress grown from acetylene	12
3.5 SEMs of CNTs vs. Ni layer thickness grown from acetylene	12
3.6 SEMs of CNTs vs. Ni layer thickness grown from methane	13
4.1 AAO templates from Al sheet	15
4.2 AAO templates from Nd-doped Al films vs. thickness	16

This Page Intentionally Left Blank

Self-Assembled Ordered Carbon Nanotube Arrays and Membranes

I. Introduction

Our goal is to develop useful, self-assembled arrays of carbon nanotubes (CNTs) with greater uniformity and smaller diameters than previously reported, as well as the first-ever free-standing membranes of vertically-aligned CNT arrays. This will be accomplished by using our thermal chemical vapor deposition (CVD) process for CNTs that results in the smallest diameter CNTs ever reported in a film in combination with a novel template method using anodized aluminum-oxide (AAO) films.

The first report of CNTs by Iijima generated great excitement.[*Nature*, 1991]. CNTs are a unique graphene-based material with intriguing physical properties and a plethora of potential applications. While most studies focus on single-wall CNTs, consisting of a single graphene layer cylinder, such materials grow at high temperature and are difficult to manipulate into useful geometries. Films are made by drying single-wall CNT-containing liquids onto a substrate; resulting morphologies look like a plate of spaghetti. This random structure limits the usefulness of such films.

Conversely, multiwall CNTs, consisting of several graphene sheets rolled into concentric cylinders, grow at lower temperatures directly onto substrates in useful configurations. We co-authored the first reports of CNT arrays on glass and Si substrates, as shown in fig. 1.1.[*Science* and *Appl. Phys. Lett.* 1998.]

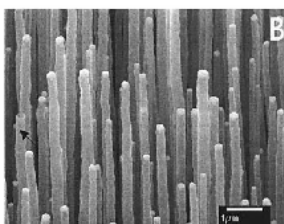


Fig. 1.1: Highly-aligned CNTs first reported by Ren, Huang, Xu, Wang, Bush, Siegal, and Provencio. [*Science*, 1998] Growth was by hot-filament assisted CVD without the use of a template.

Following our publications of aligned CNT growth, Li et al [*Appl. Phys. Lett.* 1999] reported a simpler, thermal CVD method for growing highly aligned CNTs that uses a template consisting of nanopores in anodized Al-oxide (AAO) for alignment. The advantages of this method are two-fold: (i) growth occurs in an easily controlled and scalable tube-furnace, and (ii) a close-packed hexagonal arrangement of CNTs result, as shown in fig. 1.2.

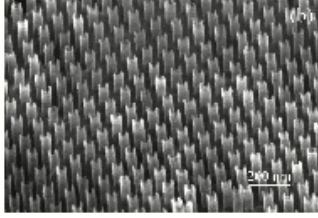


Fig. 1.2: Ordered carbon nanotube array by Li et al [Appl. Phys. Lett. 1999] grown using an AAO ordered array template of nanoholes.

While single-wall CNTs can be either semiconducting or metallic, based on tube chirality, multiwall CNTs are always conductive, expected whenever multiple graphene sheets are in parallel proximity. Aligned CNTs are ideal for numerous applications, including cold-cathode field emitters or nanoelectrodes for electrochemical and biological sensing. By opening both ends of CNTs for gas flow, arrays for nanofiltration/nanochromatography can be fabricated. These applications need CNTs with small, highly controlled diameters and individual high-crystalline quality for optimized conductivity. And while high-packing densities of CNTs are ideal for nanofiltration or nanochromatography, greater spacing between CNTs is needed for performance optimization of both field emitters and nanoelectrodes.

Controlled growth of uniform, small diameter CNTs - Several issues exist before the widespread use of CNT arrays can occur, and are illustrated in figs. 1.1 and 1.2 above. To date, fabricated CNT arrays have large outer diameters, typically ranging from 25 – 500 nm. Furthermore, these CNTs exhibit poor crystallinity. This is obvious in fig. 1 which shows non-uniform diameters along the length of individual CNTs. In addition, a wide range of diameters commonly occur between CNTs within the same sample. Non-uniform diameters both between CNTs and within a single CNT result in poor control of important properties such as conductivity and field emission. Such non-uniform diameters also limit the usefulness of CNT arrays to perform as uniform nanopores for filters. Finally, the near proximity of CNTs to one another causes shielding effects in applications such as field emitters and nanoelectrodes.

AAO templates – Several technical issues are preventing the widespread use of AAO templates for growing aligned CNT arrays. First, high-purity Al foil or sheet is typically used. Substrates need to be ultra-smooth to be useful for electronic applications. Polishing Al to roughness < 200 nm is both difficult and time intensive and, hence, expensive. In addition, Al films exhibit roughness on the order of film thickness, with facets in many directions, and as such, are not reliable templates. Second, Al anodizes rapidly, creating nanopores tens of microns deep in just a few seconds. CNTs do not easily grow to these lengths, nor are such lengths required for electronic applications. The CNT array grown from an AAO template in fig. 1.2 was both polished and etched to reveal the CNTs. And third, nanopores in AAO are hexagonal close-packed, with pore separation distances ~ the same as pore diameters. While a high pore density is preferable for filtration/chromatography applications, such close proximity between CNTs is harmful for field-emitters and nanoelectrodes due to electric field shielding effects.

II. Controlling CNT Diameters

Carbon nanotubes (CNT) are a unique form of pure graphene-based materials with intriguing physical properties and a plethora of potential applications. CNTs have created much excitement since first reported in 1991.¹ While most fundamental studies have focused on single-wall CNTs, consisting of a cylinder of a single layer of graphite, such materials grow at high temperatures and are difficult to manipulate into useful geometries. Conversely, multiwall CNTs grow at lower temperatures directly onto substrates in useful configurations.^{2,3} Multiwall CNTs consist of several graphene sheets rolled into concentric cylinders, leading to graphite-like electrical properties. The larger wall thicknesses, compared to single wall CNTs, lead to larger outer diameters, larger bore diameters, higher stiffness, and greatly improved electrical conductivity. These properties are ideal for generating nanostructures for cold-cathode electron field emission, nanoporous membranes, low-friction nanobearings, supercapacitor electrodes, ultrasensitive electrometers, and other applications.^{4,5,6,7,8} Previous work demonstrated growth of highly-aligned multiwall CNTs directly onto glass and Si substrates using plasma-enhanced hot-filament chemical vapor deposition (CVD).^{2,3}

Vacuum CVD methods involving hot-filaments and/or plasmas are difficult to control and scale for production. Li et al reported a simple thermal CVD method for growing highly-aligned CNTs that use a template consisting of pinholes in anodized Al for alignment.⁹ In our 2002 Applied Physics Letter, we reported the use of a similar thermal CVD process for growing multiwall CNTs directly on a substrate.¹⁰ We demonstrate precise control of nanotube diameters ranging from 5 – 350 nm. Since we use neither a plasma nor a template to provide alignment, CNTs grown for this study are randomly oriented. This work defines CNT growth conditions which can be applied to the use of anodized or lithographically-defined templates with predetermined pinhole sizes for growth of aligned multiwalled CNT arrays with optimal structural integrity.

To grow CNTs, we first deposit a thin Ni catalyst. Our experiments show that a minimum of ~ 3.5 nm is required for consistent CVD growth of CNTs. After cleaning Si(100) with an HF dip, followed by a DI water rinse, wafers are loaded into an RF sputter deposition system. Prior to the deposition of ~ 4 nm thick Ni deposition, a 50 nm thick W diffusion barrier is deposited to prevent unwanted Ni-silicide formation during CVD growth. Due to the large differences in thermal expansion coefficient between Si and Ni/W, the metal layers spall from the substrate during the thermal CVD process. Therefore, we deposit the metals through an Al-foil mask consisting ~ 1 mm holes, resulting in small dots of Ni/W metallization. The residual stresses arising from thermal heating are insufficient to cause spallation of such small areas. Our mask consists of 9 dots/cm².

We grow multiwall CNTs by CVD in a tube furnace at atmospheric pressure (0.8 atm in Albuquerque, NM) from a 1:9 mixture of acetylene:nitrogen gases. The Ni layer reduces by annealing in flowing CO at 600 °C for one hour. Lower temperature CO annealing appears to less effectively remove oxygen from the metal, leading to sporadic CNT growth; higher

temperatures result in amorphous carbon deposition. Following this oxide reduction, the tube furnace is flushed with N₂ and the temperature raised to that desired for CNT growth. Once the desired growth temperature is reached, the furnace is flushed with the gas mixture used for the growth ambient. All CNT samples for this study grew in 15 minutes. We studied growth at temperatures ranging from 630 – 830 °C. At the end of the prescribed growth period, the furnace is flushed with N₂ and furnace-cools to < 100 °C in ~ 1 hour. Growth above 790 °C yields micron-sized diameter tubular-like cluster structures from the gas phase, independent of the catalyst, that coat the inside of the furnace apparatus, including the substrate. We are currently studying growth below 630 °C and will report the results later.

Figure 2.1 shows scanning electron microscopy (SEM) images for CNT samples grown at temperatures ranging from 630 – 790 °C. Nanotube formation is very uniform over the entire metallized sample areas, in terms of diameters, lengths, and areal coverage. In addition, the majority of CNTs have very few kinks and bends. As expected, these CNTs grow without any preferred orientation. To accurately measure diameters < 25 nm, we use transmission electron microscopy (TEM). Figure 2.2 plots the CNT diameters vs. growth temperature. The results fit an exponential function. SEM and TEM measurements are identical, within an error bar the size of the data points, for CNTs grown above 700 °C. TEM finds smaller sizes for CNTs grown at temperatures below 700 °C, due to its superior resolution compared to SEM. TEM finds that the walls of the smallest-diameter CNTs demonstrate superb long-range order. Such order is present in most of the tubes grown at temperatures below ~750 °C, however, only for the innermost walls with diameter < 5 nm. The outer walls, those with diameter > 5 nm, of CNTs consist primarily of nanocrystalline carbon with only short-range order. These nanostructural studies will be described in detail elsewhere.

These results demonstrate precise control of CNT diameters from 5 – 350 nm as an exponential function of growth temperature. Other studies report CNT diameter control, although typically over a much smaller size range, and rarely as small as 5 nm.^{11,12} These reports typically associate control of CNT diameters with the grain size of the metal catalyst used. To first order, this is likely correct for our study as well. By annealing the Ni film in N₂ to the growth temperature, the film likely coalesces into small islands on top of the underlying W layer. Additionally, the presence of the W layer may provide a thermodynamic stimulus for highly-controlled Ni-island formation due to differences in surface free energies compared to substrate surfaces used in other reports. More study is required on this topic.

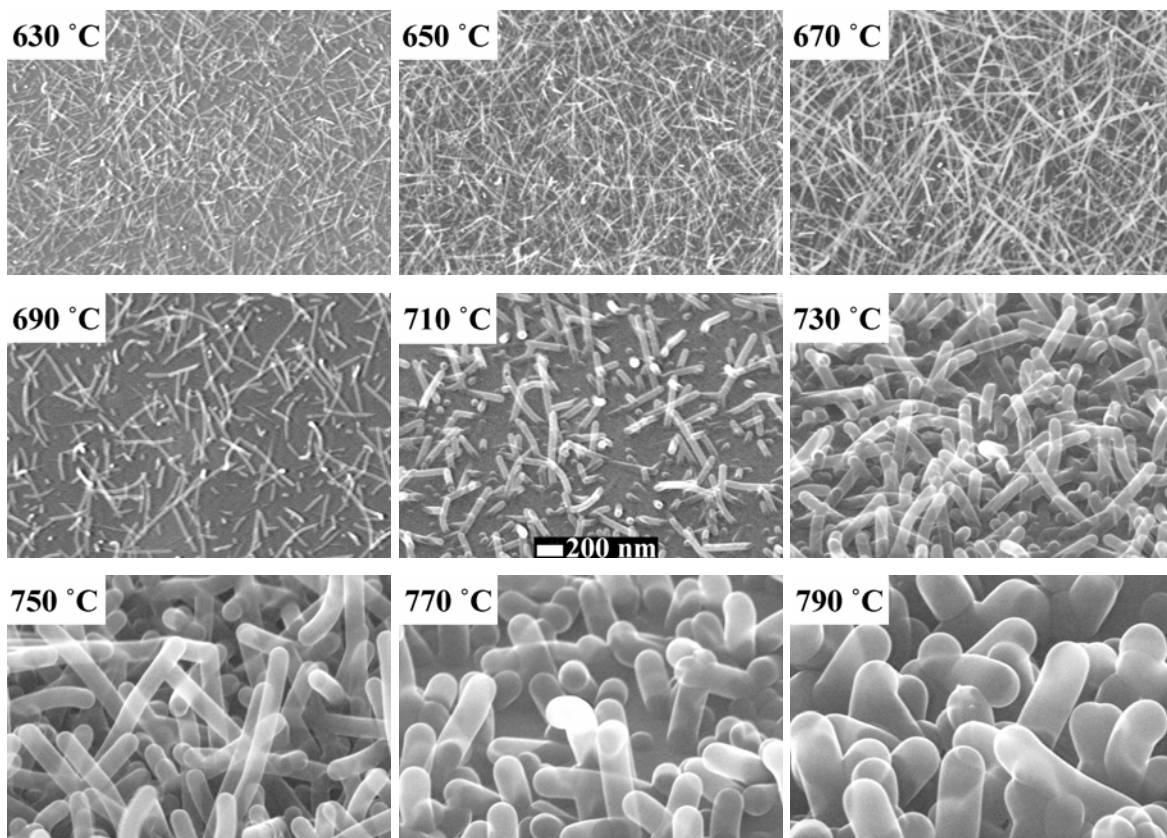


Figure 2.1: SEM images of CNT films grown at temperatures ranging from 630 – 790 °C.

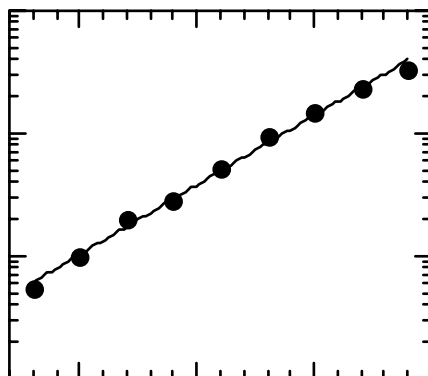


Figure 2.2: CNT outer diameters vs. growth temperatures.

We used Rutherford backscattering spectrometry (RBS) with 2.0 MeV $^4\text{He}^+$ ions to further study the deposition of carbon by thermal CVD, and to confirm the presence of Ni in the samples. Figure 2.3 is the RBS spectrum for the sample grown at 690 °C. The areal density of Ni atoms, determined by comparing the ratio of the Ni integrated intensity to the W integrated intensity, is constant to $\pm 3\%$ for all the samples following CNT growth, confirming that Ni does not volatilize via some reaction with the acetylene at the temperatures or growth times used in this study. The C atom areal density can be calculated from an RBS spectrum two different ways.¹³ The first method involves measuring the integrated intensity under the C portion of the spectrum. This is shown in the insert of fig. 2.3. Clearly, the backscattered signal from C atoms is very weak compared to the signal from the underlying Si substrate, leading to measurements with a high degree of error.

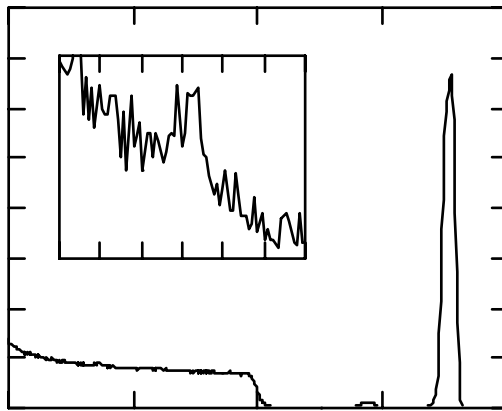


Figure 2.3: A typical RBS spectrum for CNT/Ni/W/Si(100). This sample grew at 690 °C. The insert is an expanded view of the small box showing the C peak.

We more accurately measure the energy shift of the W RBS surface edge due to a C elemental absorber grown on top of it compared to an as-deposited W film with no C growth. We choose the W surface edge rather than the Ni or Si edges since the W layer is the most likely to remain pristine. This measurement is independent of the density of the layers, and the determination of the W surface edge is precise to within ± 2 keV, corresponding to $\pm 0.65 \times 10^{16}$ C atoms/cm². Results from this second determination of the areal density of C atoms as a function of growth temperature are shown in Figure 4. Note that RBS measurements do not distinguish carbon atoms that are part of the nanotubes from those that may be present as amorphous carbon byproducts. Nevertheless, the excellent exponential fit to this data suggests that the deposition of carbon atoms from thermal CVD using acetylene is a thermally activated process. As an aside, we note that the values calculated from the C peak method agree very well with those presented in fig. 2.4, however, with significantly more scatter in the data.

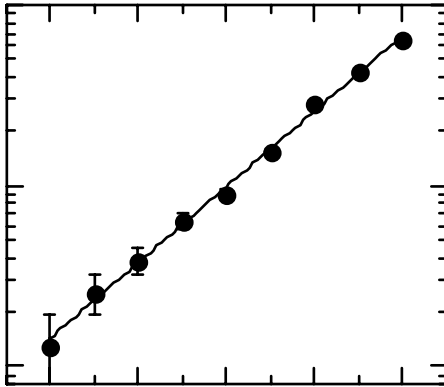


Figure 2.4: Carbon atom areal density vs. growth temperature measured from the shift in the W surface edge from RBS.

In summary, the diameter of CNTs, and the total deposition of carbon material, are exponential functions of the growth temperature used in a thermally-activated CVD process using acetylene with a Ni catalyst. This growth method is extremely self-consistent, and allows the controlled growth of CNTs with uniform diameters ranging from 5 – 350 nm. CNTs grown at 630 °C demonstrate long-range structural perfection in the nanotube walls. CNTs grown at higher temperatures have highly-disordered nanocrystalline graphite walls surrounding a highly-ordered innermost wall structure. Detailed nanostructural study of these CNTs as a function of growth temperature will be presented elsewhere.

Sandia is a multiprogram laboratory operated by Sandia Corp., a Lockheed Martin Co., for the US DOE under contract No. DE-AC04-94AL85000. The authors thank D. R. Tallant and J. C. Barbour for providing meaningful insights, and F. H. Kaatz for helping set up the growth apparatus.

References:

- ¹ S. Iijima, *Nature*, **354**, 56 (1991).
- ² Z. F. Ren, Z. P. Huang, J. W. Xu, P. Bush, M. P. Siegal, and P. N. Provencio, *Science*, **282**, 1105 (1998).
- ³ Z. P. Huang, J. W. Xu, Z. F. Ren, J. H. Wang, M. P. Siegal, and P. N. Provencio, *Appl. Phys. Lett.* **73**, 3845 (1998).
- ⁴ W. A. De Heer, A. Chatelain, and D. Ugarte, *Science* **270**, 1179 (1995).
- ⁵ M. B. Shiflett and H. C. Foley, *Science* **285**, 1902 (1999).
- ⁶ J. Cummings and A. Zettl, *Science* **289**, 602 (2000).
- ⁷ E. Frackowiak, K. Metenier, V. Bertagna, and F. Beguin, *Appl. Phys. Lett.* **77**, 2421 (2000).
- ⁸ L. Roschier, R. Tarkiainen, M. Ahlskog, M. Paalanen, and P. Hakonen, *Appl. Phys. Lett.* **78**, 3295 (2001).
- ⁹ J. Li, C. Papadopoulos, J. M. Xu, and M. Moskovits, *Appl. Phys. Lett.* **75**, 367 (1999).
- ¹⁰ M. P. Siegal, D. L. Overmyer, and P. P. Provencio, *Appl. Phys. Lett.* **80**, 2171 (2002).
- ¹¹ Y. C. Choi, Y. M. Shin, Y. H. Lee, B. S. Lee, G.-S. Park, W. B. Choi, N. S. Lee, and J. M. Kim, *Appl. Phys. Lett.* **76**, 2367 (2000).
- ¹² C. J. Lee, J. Park, Y. Huh, and J. Y. Lee, *Chem. Phys. Lett.* **343**, 33 (2001).
- ¹³ W.-K. Chu, J. W. Mayer, and M.-A. Nicolet, “Backscattering Spectrometry”, (Academic Press, New York, 1978).

III. Controlling the Site Density of Multiwall CNTs

There is great interest in developing carbon nanotube (CNT) films with useful geometries. Multiwall CNTs readily grow on substrate surfaces from one of several variations of chemical vapor deposition (CVD), all involving the use of metal catalysts, and typically result in high (10^{10} CNTs/cm²) site densities, corresponding to an average spacing ~ 100 nm.^{1,2,3} Potential applications that require significant spacing between CNTs include cold-cathode field emitters for flat-panel displays^{4,5,6}, electron beam lithography^{7,8}, and x-ray tubes^{9,10}, and nanoelectrodes for capacitors^{11,12} and electrochemical sensors¹³. For example, field emission appears to optimize at densities near 10^7 CNTs/cm², which is an average spacing of a few microns.¹⁴ Nanoelectrodes have a similar requirement. In both cases, it is due to the screening effects of applied electric fields from close-packed CNTs.

Several papers report control of CNT density, usually for field emission measurements. One simply harvests CNTs from bulk preparation methods, disperses them in solution to a known concentration, and dip coats them onto a given substrate surface.⁴ However, this results in tangled webs of curly CNTs. Others involve either dispersal of catalytic metal particles by sol-gel or electrochemistry, or lithography of a catalyst film to control the density of CVD grown CNTs.^{15,16,17,18} While highly effective, each variation has additional processing steps. Finally, another allows the metal catalyst to diffuse into an imperfect barrier layer, designed to prevent reaction with the substrate, reducing the amount of metal available to act as a catalyst to result in dense CNT clusters with somewhat controlled spacing.¹⁹ However, distribution of individual CNTs was not observed and the method is likely difficult to control.

We reported two distinct methods to control individual CNT density directly during thermal CVD growth.²⁰ The first selects the hydrocarbon source gas based on its chemical reactivity. The second controls the residual stress of the metal catalyst/diffusion barrier film layers. These methods are combined to provide reliable control of the average spacing between CNTs.

CNT growth is described elsewhere.²¹ Briefly, a 50-nm-thick W diffusion barrier followed by a thin Ni catalyst are rf-sputtered in argon onto HF-dipped Si(100) substrates through an Al-foil shadow mask with ~ 1 mm diameter holes, resulting in 9 dots/cm² of Ni/W metallization. The dots prevent spallation from stresses arising during thermal CVD growth due to the thermal expansion coefficient differences between W and Si. The samples are heated in a tube furnace to 600 °C for 1 h in flowing CO at atmospheric pressure (0.8 atm in Albuquerque, NM) to reduce the Ni layer. The ambient is flushed with N₂, the temperature ramped to that desired for CNT growth, and then flushed with the CVD growth ambient (~ 10 % hydrocarbon : 90% N₂). For this study, CNTs grow at 650 °C for 15 min, resulting in relatively straight and uniform 10 nm diameters.

Four hydrocarbon gases are studied: C₂H₂ (acetylene), C₂H₄ (ethylene), and C₂H₆ (ethane), which have a C-C triple, double, and single bond, respectively, and CH₄ (methane). The

chemical reactivity of these compounds are related to their heats of formation, obtained from a *CRC Handbook of Physics and Chemistry*, and shown in Fig. 3.1. In general, the greater the bond number, the more reactive. Therefore, the reactivity of acetylene > ethylene > ethane. With negative heats of formation, both ethane and methane are the least reactive, with ethane slightly less than methane. Fig. 3.2 shows scanning electron microscopy (SEM) images of CNT films grown using these hydrocarbons from 5-nm-thick Ni catalyst films, where both the Ni and W were deposited in $p(\text{Ar}) = 20 \text{ mT}$. The resulting CNT site densities are in the same order as the chemical reactivity of the hydrocarbons. No CNTs are found for ethane, the least reactive gas studied, although this may be related to the relatively high stress of the metal layers, discussed below. The average separation between CNTs grown using acetylene, ethylene, and methane is $\sim 30 \text{ nm}$, 100 nm , and $1 \mu\text{m}$, respectively, yielding site densities on the order of 10^{11} , 10^{10} , and 10^8 CNTs/cm^2 . By selecting the appropriate chemically-reactive hydrocarbon gas, several orders of magnitude of CNT site density control is achieved.

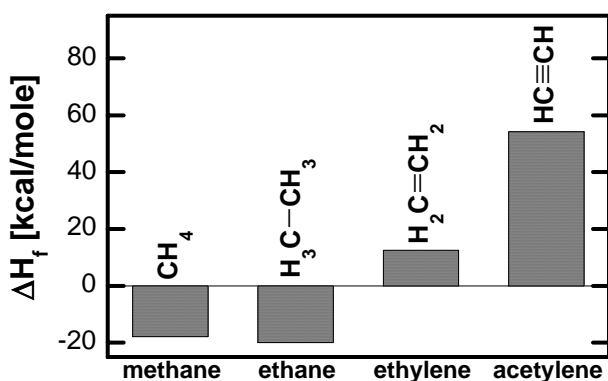


Figure 3.1: Heat of formation of various hydrocarbon gases.

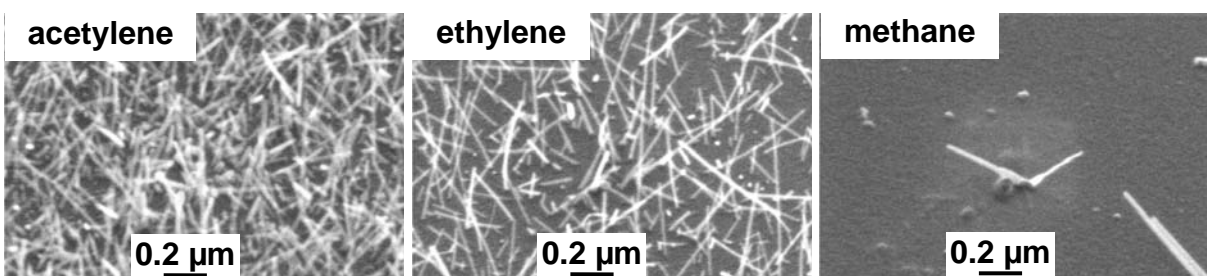


Figure 3.2: SEM images of CNTs grown using identical conditions except for the choice of hydrocarbon gas.

Further control of the CNT density can be achieved by altering the residual stress of the Ni/W film during sputter deposition. Stress is determined by measuring the change in curvature of a 2-inch Si(100) wafer with a stylus profilometer before and after deposition of 100-nm-thick

films, measured separately for both W and Ni. Since stress is proportional to film thickness, fig. 3.3 plots the tensile film stress of W and Ni scaled to 50- and 10-nm-thick films, respectively, grown in $p(\text{Ar})$ ranging from 8 to 80 mT. In general, W film stress increases with decreasing $p(\text{Ar})$, with buckling occurring near $p(\text{Ar}) = 10$ mT. W films grown in $p(\text{Ar}) = 40 - 80$ mT are slightly compressive and essentially equivalent. Ni residual film stress is tensile in the range studied and much lower than that of W in low $p(\text{Ar})$, however, note that it dominates the total film stress for the combined layers when grown in $p(\text{Ar}) \approx 15$ mT. The Ni stress increases with increasing $p(\text{Ar})$, and is essentially equivalent from 25 – 80 mT.

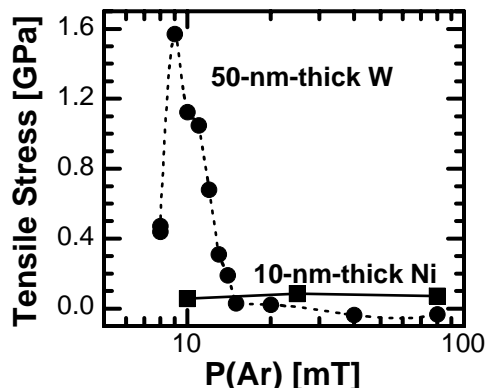


Figure 3.3: Residual stress of W and Ni films as a function of $p(\text{Ar})$ used during sputter deposition.

To test the relevance of stress for CNT density, 10-nm-Ni/50-nm-W at 40, 20, and 10 mT are deposited onto Si(100). Fig. 3.4 shows SEM images for the resulting CNTs grown using acetylene. From 40 to 20 mT, there is little variation in the Ni tensile stress, however, the W stress increases measurably, resulting in a modest decrease in the CNT site density from $10^{11} - 10^{10}$ CNTs/cm². However, substantial stress exists in the W film at 10 mT; the density decreases to $\sim 10^8$ CNTs/cm². Unfortunately, this dramatic decrease is associated with a severe degradation of the W/Ni surface, caused by stress relaxation at the 650 °C CNT growth temperature.

The most dramatic variation in stress, and hence CNT density, is between 10 and 15 mT. Despite successfully growing CNTs exhibiting different densities from metals deposited in 1 mT intervals in this range, such precision is difficult to achieve. Alternatively, since the W stress is negligible at $p(\text{Ar}) = 40$ mT, the Ni stress can be accurately controlled by thickness. Fig. 3.5 shows SEM images of CNTs grown from Ni catalyst layers 2.5, 7.5, 12.5, and 20 nm thick, resulting in densities of $\sim 1 \times 10^{11}$, 2×10^{10} , 3×10^9 , and 0 CNTs/cm², respectively. Consistent results were also obtained for 5 and 10 nm thick Ni films. Inspecting the substrate surface beneath the CNTs reveals increasing roughness with increasing Ni thickness, or residual stress, similar to simply changing the metal layer stress as shown in fig. 3.4. A similar result was published for rf plasma-enhanced CVD growth at 650 °C, using thermally evaporated Ni catalyst films.²² Their interpretation is that thicker Ni films generate larger Ni islands that do not

support CNT growth. However, CNTs grown from similar catalyst films at higher temperatures, presumably resulting in larger Ni islands, simply have larger diameters.²¹ Therefore, the Ni thickness result reported is perhaps also due to film stress, which should impact the geometry of a given Ni island.

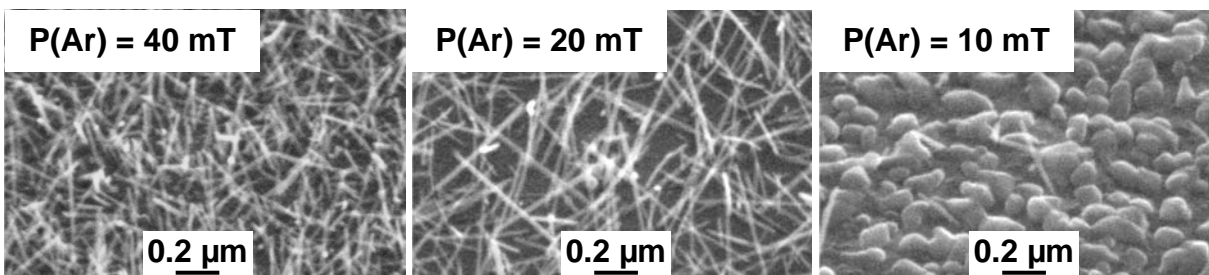


Figure 3.4: SEM images of CNTs grown on 10-nm-thick Ni/50-nm-thick W/Si(100) with different stress levels controlled by p(Ar).

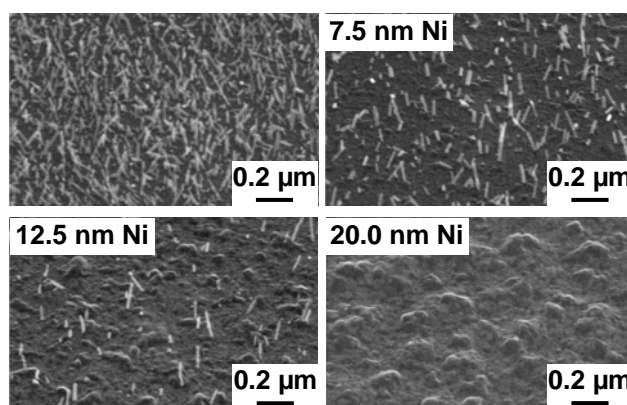


Figure 3.5: SEM images of CNTs grown using acetylene with stress controlled by the Ni film thickness.

By combining the concepts of chemical reactivity and film stress, density can be further controlled by using a hydrocarbon gas with lower reactivity. Fig. 3.6 shows CNTs grown using methane from the same metal substrates as above. Here, Ni film thicknesses of 2.5, 7.5, 12.5, and 20 nm result in densities of $\sim 2 \times 10^{10}$, 4×10^8 , 4×10^7 , and 0 CNTs/cm². Changing the hydrocarbon from acetylene to methane lowers the CNT site densities 1 – 2 orders of magnitude for the same catalyst/diffusion barrier films.

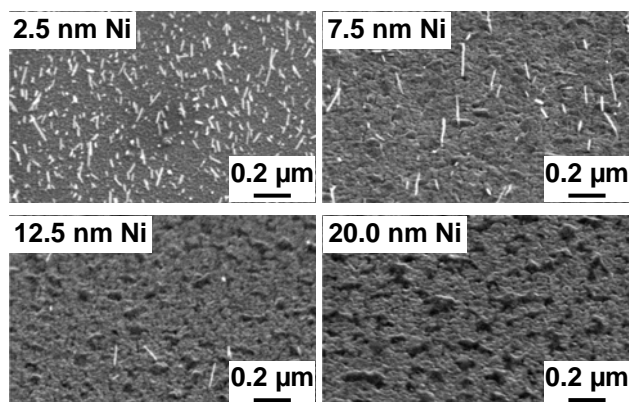


Figure 3.6: SEM images of CNTs grown using methane with stress controlled by the Ni film thickness.

In summary, we demonstrate that the CNT site density can be directly controlled by the thermal CVD growth conditions employed: first, by selecting the hydrocarbon gas based on its heat of formation, or chemical reactivity; and second, by controlling the residual stress of the catalyst/diffusion barrier layers. Combining these methods, 4 orders of magnitude of CNT density control is obtained. Use of other hydrocarbons and/or slightly higher metal layer stresses can likely expand that range to considerably lower site densities.

References

- 1 T. Kyotani, L-f. Tsai, and A. Tomita, *Chem Mater.* **8**, 2109 (1996).
- 2 Z. F. Ren, Z. P. Huang, J. W. Xu, J. H. Wang, P. Bush, M. P. Siegal, and P. P. Provencio, *Science* **282**, 1105 (1998).
- 3 Z. P. Huang, J. W. Xu, Z. F. Ren, J. H. Wang, M. P. Siegal, and P. P. Provencio, *Appl. Phys. Lett.* **73**, 3845 (1998).
- 4 J-M. Bonard, J-P. Salvetat, T. Stockli, W. A. de Heer, L. Forro, and A. Chatelain, *Appl. Phys. Lett.* **73**, 918 (1998).
- 5 Q. H. Wang, A. A. Setlur, J. M. Lauerhaas, J. Y. Dai, E. W. Seelig, and R. P. H. Chang, *Appl. Phys. Lett.* **72**, 2912 (1998).
- 6 W. B. Choi, D. S. Chung, J. H. Kang, H. Y. Kim, Y. W. Jin, I. T. Han, Y. H. Lee, J. E. Jung, N. S. Lee, G. S. Park, and J. M. Kim, *Appl. Phys. Lett.* **75**, 3129 (1999).
- 7 H. Dai, N. Franklin, and J. Han, *Appl. Phys. Lett.* **73**, 1508 (1998).
- 8 K. B. K. Teo, M. Chhowalla, G. A. J. Amaratunga, W. I. Milne, P. Legagneux, G. Pirio, L. Gangloff, D. Pribat, V. Semet, V. T. Binh, W. H. Bruenger, J. Eichholz, H. Hanssen, D. Friedrich, S. B. Lee, D. G. Hasko, and H. Ahmed, *J. Vac. Sci. Technol.* **B 21**, 693 (2003).
- 9 H. Sugie, M. Tanemura, V. Filip, K. Iwata, K. Takahashi, and F. Okuyama, *Appl. Phys. Lett.* **78**, 2578 (2001).
- 10 G. Z. Yue, Q. Qiu, B. Gao, Y. Cheng, J. Zhang, H. Shimoda, S. Chang, J. P. Lu, and O. Zhou, *Appl. Phys. Lett.* **81**, 355 (2002).
- 11 E. Frackowiak, K. Metenier, V. Bertagna, and F. Beguin, *Appl. Phys. Lett.* **77**, 2421 (2000).
- 12 J. H. Chen, W. Z. Li, D. Z. Wang, S. X. Yang, J. G. Wen, and Z. F. Ren, *Carbon*, **40**, 1193 (2002).
- 13 Y. Tu, Y. Lin, and Z. F. Ren, *Nano Lett.* **3**, 107 (2003).
- 14 L. Nilsson, O. Groening, C. Emmenegger, O. Kuettel, E. Schaller, L. Schlapbach, H. Kind, J-M. Bonard, and K. Kern, *Appl. Phys. Lett.* **76**, 2071 (2000).
- 15 J. Kind, J-M. Bonard, L. Forro, K. Kern, K. Hernadi, L-O. Nilsson, and L. Schlapbach, *Langmuir* **16**, 6877 (2000).
- 16 Y. Tu, Z. P. Huang, D. Z. Wang, J. G. Wen, and Z. F. Ren, *Appl. Phys. Lett.* **80**, 4018 (2002).
- 17 Z. F. Ren, Z. P. Huang, D. Z. Wang, J. G. Wen, J. W. Xu, J. H. Wang, L. E. Calvet, J. Chen, J. F. Klemic, and M. A. Reed, *Appl. Phys. Lett.* **75**, 1086 (1999).
- 18 Z. P. Huang, D. L. Carnahan, J. Rybczynski, M. Giersig, M. Sennett, D. Z. Wang, J. G. Wen, K. Kempa, and Z. F. Ren, *Appl. Phys. Lett.* **82**, 460 (2003).
- 19 K. B. K. Teo, M. Chhowalla, G. A. J. Amaratunga, W. I. Milne, G. Pirio, P. Legagneux, F. Wyczisk, D. Pribat, and D. G. Hasko, *Appl. Phys. Lett.* **80**, 2011 (2002).
- 20 M. P. Siegal, D. L. Overmyer, and F. H. Kaatz, *Appl. Phys. Lett.* **84**, 5156 (2004).
- 21 M. P. Siegal, D. L. Overmyer, and P. P. Provencio, *Appl. Phys. Lett.* **80**, 2171 (2002).
- 22 L. Valentini, J. M. Kenny, L. Lozzi, and S. Santucci, *J. Appl. Phys.* **92**, 6188 (2002).

IV. AAO Template Formation

Some form of structural template is required to achieve vertical alignment for arrays of CNTs using thermal CVD. Al anodization is simple, inexpensive, and readily scaleable, as is the electrodeposition of metal catalysts (Ni, Co, or Fe) into the nanopore wells. The CNT array shown in fig. 1.2 was made precisely in this manner. We plan to implement two major improvements. First, since we can grow significantly smaller CNTs than reported by other groups, we require AAO templates with smaller diameter nanopores. Fig. 4.1 shows that nanopore diameters can be controlled by varying the anodization potential and solution composition. These AAO materials were fabricated using thin Al sheet. While Al itself is inherently inexpensive, polishing an Al surface to a mirror-finish is very time-consuming, and therefore, costly. Furthermore, it is essentially impossible to achieve an atomically-smooth surface by polishing such a soft material. Fig. 4.1(b) shows a ridge in the lower left corner of the image.

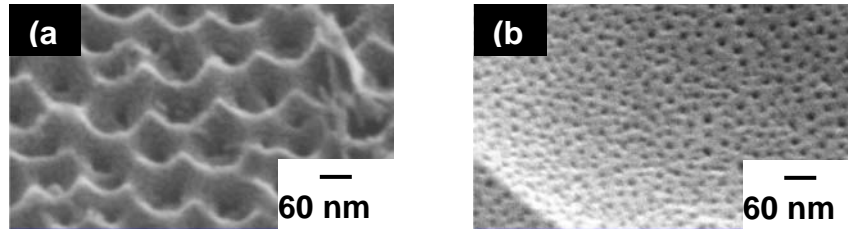


Figure 4.1: AAO templates from Al sheet with (a) 50 nm and (b) 10 nm nanopore diameters.

Second, the depth of these nanopores typically are tens of microns. Since CNTs grown with our thermal CVD process are typically 0.1 – 2 microns long, use of such deep pores for a template is overkill, and its use likely will slow down the kinetics of CNT growth due to diffusion limitations into such deep pores. A solution to these problems would be to use Al films grown onto a smooth substrate, such as Si. The thickness of the Al film would control the nanopore depth. And no polishing would be needed. Unfortunately, Al films do not grow mirror-smooth. Rather, they tend to be polycrystalline materials with grains of many different sizes. Typically, Al films grown by physical methods such as evaporation or sputtering are about as rough as they are thick. The existing large grain boundaries create surfaces within the thickness of the films, allowing the Al to oxidize through nearly its entire film thickness uncontrollably upon exposure to ambient air.

We have been able to show that by doping Al films with rare-earth elements, such as Nd, mirror-smooth films can be achieved by sputter deposition. Careful control of the rf sputter conditions even allow the Nd-doped Al films to grow on Si(100) at room temperature with negligible residual stress. This allows the deposition of Al films with nearly any thickness. Indeed, we have already grown some films $> 7 \mu\text{m}$ thick on Si. These films show no evidence of stress, and are mirror-smooth. The ability to grow such material creates an ideal candidate for use as a template for CNT growth, if they can be anodized controllably.

Fortunately, Nd-doped Al films anodize similar to bulk Al. This new AAO process provides extremely uniform substrates to form the templates. The AAO films shown in fig. 4.2 were anodized using the exact same conditions as that shown above in fig. 1(a) from a bulk Al sheet. These AAO template pore diameters of 50 nm, result in an array density approaching 10^{10} nanopores/cm². These films were all anodized in phosphoric acid with a 60 V potential. Furthermore, readily-achievable 10-nm pore diameters will provide array densities $> 10^{11}$ nanopores/cm². Each nanopore is a template for a vertically-aligned CNT grown by CVD.

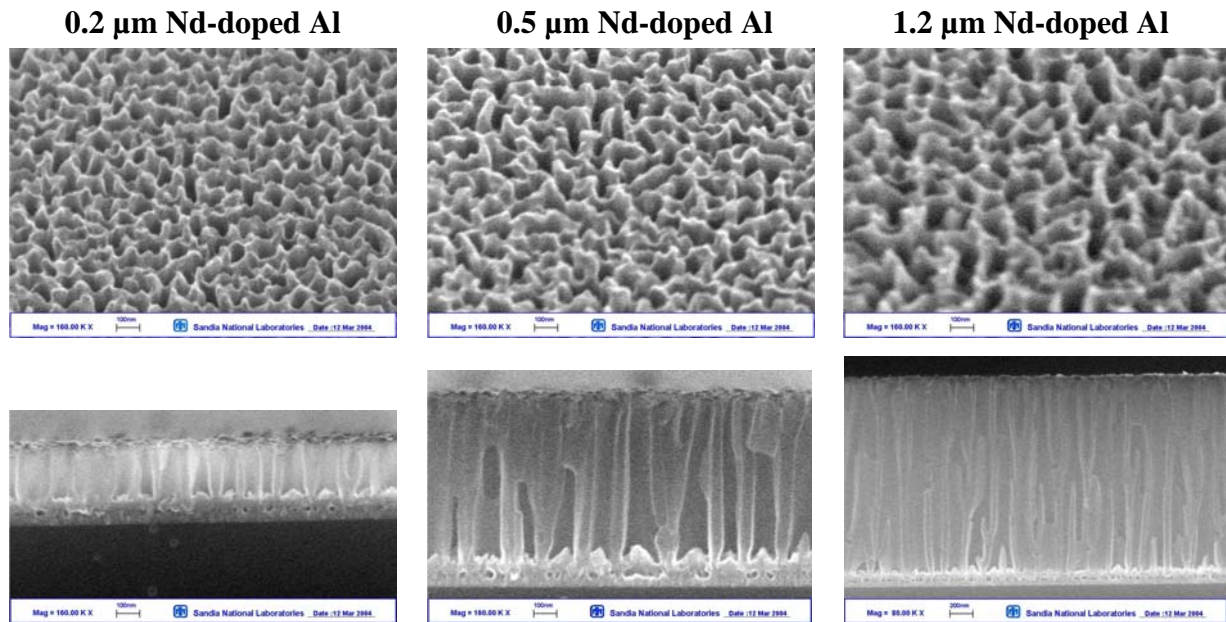


Figure 4.2: AAO vs. Nd-doped Al film thickness.

Using mirror-smooth Nd-doped Al films, we will be able to fabricate controlled nanopore arrays with defined depths. These AAO nanopore arrays will be used as a template for aligned CNT growth onto useful, cost-effective substrates such as Si or glass. By correlating nanopore diameters and anodization conditions, we will create AAO templates with the appropriate pore size for a given CNT diameter, providing the best possible structural support. To date, we are the only group to demonstrate controlled CNT film growth with diameters < 20 nm. We expect to produce CNT arrays in AAO templates with diameters ranging from 3 – 100 nm due to our thermodynamic understanding of the nanotube growth process.

The next step in the process for using these AAO films as templates has been taken. Ni has been successfully electrochemically deposited into the bottoms of the nanopores. Ni, or some transition metal such as Co or Fe, is required to act as a catalyst for CNT growth. We have not yet grown CNTs in these templates.

V. Summary

This ambitious project had three main goals. First, anodized aluminum-oxide (AAO) templates were to be fabricated from the deposition of thick Al films on Si substrates. Second was the determination of spacing methods for the growth of carbon nanotubes (CNTs) on a substrate surface. Many potential applications require significant spacing between individual CNTs. Third was the growth of CNT arrays in AAO templates, to be followed by CNT membrane fabrication.

No other group has reported the growth of several micron thick Al films on any substrate, due to the development of high residual stress and rough film morphology, never mind using them for conversion into AAO. However, we have learned to grow such thick, mirror-smooth films by using both a thin adhesion layer, rare-earth doping, and unique rf-sputter deposition conditions that greatly lower the kinetic energy of the depositing species, effectively eliminating the development of residual stress. This room-temperature, stress-free physical deposition of Al has many other potential applications to create AAO templates for extremely high aspect ratio CNTs and nanowires of other materials. In addition, the method has been extended to other elemental films, such as carbon for nanoporous-carbon growth for sensor applications, boron for thick films for neutron detection, and W and Ir metals for various other projects.

In addition, we have shown that stress-free Al films can be anodized very uniformly, and that the lateral dimensions of pore development are not dependent on the thickness of the Al film. This provides independent control of the template length for CNT/nanowire growth from other growth parameters controlling diameters, spacings, etc. A new project and other new collaborations have already resulted from this achievement alone.

Two complementary methods were identified to control the spacing between CNTs on a substrate surface as a function of growth conditions without any additional processing. Combined, they yield more than 4 orders-of-magnitude control over CNT areal site density. The first method shows that the site density varies with the heat of formation of the hydrocarbon gas used during CNT growth by chemical vapor deposition. The second method demonstrates that the site density decreases with increasing residual stress of the metal catalyst/diffusion barrier layers. This latter method is possible only by our understanding the mechanism to relieve metal stress during sputter deposition as described above.

The final major milestone was only partially completed. Ni metal catalysts have been electrochemically deposited into AAO templates grown on Si substrates for the first time. Previously, only bulk AAO templates have been used because of the inability to grow thick, mirror-smooth Al films, which we have overcome. Initial studies of CNT growth into these templates are promising, but incomplete at this time. Clearly, this also prevents our attempt to create free-standing CNT membranes. Given how close the project came to full fruition, it is likely that these final milestones will be achieved shortly after the end of this project.

VI. Publications, Presentations and Patent Disclosures

This section lists publications and presentations resulting from this project.

Publications

“Controlling the site density of multiwall carbon nanotubes via growth conditions,” M. P. Siegal, D. L. Overmyer, and F. H. Kaatz, *Appl. Phys. Lett.* **84**, 5156 (2004).

Presentations

“Controlling the site density of carbon nanotubes on a substrate surface via growth methods,” *M. P. Siegal* and D. L. Overmyer, Meeting of the Electrochemical Society, San Antonio, TX, May 9 – 14, 2004.

Sandia Patent Disclosures

“Ordered carbon nanotube membranes,” M. P. Siegal, W. G. Yelton, and D. R. Tallant, Nov. 4, 2003, SD-7610/S-103,470.

Distribution List

Copies	Mail Stop	Name	Org.
1	123	LDRD Office, Donna Chavez	1011
3	1421	Michael P. Siegal	1126
1	1421	Donald L. Overmyer	1126
1	1421	Paula Provencio	1111
1	1421	George A. Samara	1130
1	601	Bob Biefeld	1126
1	1056	Barney Doyle	1111
1	1425	Graham Yelton	1743
1	603	Jim Hudgens	1743
1	344	Adam Rowen	1743
2	899	Technical Library	9616
1	9018	Central Technical Files	8945-1